Open Access Library Journal
2023, Volume 10, e9550
ISSN Online: 2333-9721
ISSN Print: 2333-9705

Double Folding Potential and the Deuteron-Nucleus Inelastic Scattering in the Optical Model Framework

Raymond C. Abenga[1]*, Yahaya Yola Ibrahim[2], Idris Dauda Adamu[2]

[1]Department of Pure and Applied Physics, Veritas University, Abuja, Nigeria
[2]Department of Physics, Bayero University, Kano, Nigeria
Email: *abengar@veritas.edu.ng

How to cite this paper: Abenga, R.C., Ibrahim, Y.Y. and Adamu, I.D. (2023) Double Folding Potential and the Deuteron-Nucleus Inelastic Scattering in the Optical Model Framework. *Open Access Library Journal*, **10**: e9550.
https://doi.org/10.4236/oalib.1109550

Received: November 8, 2022
Accepted: April 10, 2023
Published: April 13, 2023

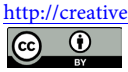

Abstract

The observed angular distribution data of deuteron elastic and inelastic scattering from ^{58}Ni at 170 MeV, ^{70,72}Ge, ^{90}Zr, ^{116}Sn at 171 MeV and ^{208}Pb at 86 MeV are analyzed within the optical model framework. The real and imaginary parts of the optical potentials were calculated using the double folding procedure with a B3Y-Fetal effective interaction. The obtained potentials are fitted with appropriate Woods-Saxon form factors and introduced into the DWUCK4 code to calculate the inelastic scattering cross sections. The calculated cross-sections are found to be in good agreement with experimental data. A satisfactory fit of the angular distribution data of the theoretical calculation to experimental data was achieved in both the elastic and inelastic channels.

Subject Areas

Modern Physics

Keywords

Effective Interaction, DWBA, DWUCK4, Double Folding Model, Optical Potential, Woods-Saxon Form Factor

1. Introduction

One of the simplest ways to investigate and obtain information about the excited state of a nucleus is through inelastic scattering analysis when it is bombarded with a nucleon or nucleus of a light ion [1]. This investigation is geared towards providing the most suitable potential form that explains the experimental data of

nuclear reactions [2]. It has long been advocated that heavy-ion (HI) optical potentials determined through elastic scattering could be tested in non-elastic channels. The call for the use of the optical potentials of the HI determined in the elastic channel was motivated by the fact that optical potentials are capable of reproducing scattering cross-sections for other reaction channels [3].

Scattering cross-sections are studied by analyzing the angular distribution data of nuclear reactions in the elastic channel by using phenomenological optical potentials or potentials obtained through folding models [4] [5] [6] [7]. The phenomenological potentials are extensively used but are however found to be ambiguous and difficult to use due to the large number of adjustable parameters that are to be controlled to obtain a good fit of the theoretical calculations to the experimental data. However, in recent years a good description of scattering cross-section data has been achieved by relating optical potentials to those obtained using an effective nucleon-nucleon (NN) interaction in the double folding model (DFM) framework [8]. The complexity of the phenomenological potentials necessitated the development of semi-microscopic potentials.

The double folding (DF) potential has been found appropriate for use in the optical model (OM) due to its simple approach and the absence of ambiguities that are associated with the phenomenological potentials [9]. The DF potentials are therefore alternatives to the phenomenological potentials and have been used over the years to construct the real part of the optical potential (OP) for optical model analysis with the imaginary part taken phenomenologically [10]. Due to the success achieved in the use of the double folding model in the description of scattering data in the elastic channel, the model has received considerable attention and recommendation over the years for its use in non-elastic channels [11] [12] [13].

Following this interest and recommendation, the DFM was used to study deuteron-nucleus and other nucleus-nucleus scattering processes. In these studies, the real parts of the optical potentials were constructed using the DF procedure while the imaginary parts were taken phenomenologically [12] [13] [14] [15] [16]. As an extension of these works, DFM is used in this study to determine both the real and the imaginary parts of the optical potentials for the deuteron-nucleus inelastic scattering analysis. In this work, an effective interaction termed B3Y-Fetal is used in the double folding calculation. The inelastic scattering cross-section data of six targets namely: ^{58}Ni at 170 MeV, ^{70,72}Ge, ^{90}Zr, ^{116}Sn at 171 MeV and ^{208}Pb at 86 MeV are analyzed.

2. Theoretical Formalism

In this section, the formalism to the construction of the optical potential using the double folding model for the deuteron-nucleus inelastic scattering analysis is discussed. The formulation of the distorted wave Born approximation (DWBA) method as included in the DWUCK4 code for numerical calculations is also presented.

2.1. The Optical Potential

The strengths of the optical potentials of the present calculations are derived using the double folding model by convoluting an effective nucleon-nucleon interaction with the ground state density distributions of the projectile and target nuclei [17]. The DF potential $V_F(r)$ is obtained by averaging an appropriate NN interaction over the density distributions of the interacting nuclei. In its simplest form, the DF potential is written as [18] [19],

$$V_F(r) = \iint \rho_1(r_1)\rho_2(r_2)V_{NN}(r - r_1 + r_2)\mathrm{d}r_1\mathrm{d}r_2, \tag{1}$$

where V_{NN} is an effective NN interaction and $\rho_i(r_i)$ are the density distributions of the projectile and target nuclei ($i = 1, 2$).

The effective NN interaction has been used extensively in the studies of nuclear matter properties and the one under consideration in this work is the B3Y-Fetal interaction. The details of this interaction and its derivation are discussed in [20] [21] [22]. The B3Y-Fetal interaction is composed of two terms namely: the direct and the exchange parts. However, the approximation in which the effective interaction V_{NN} is written as the direct part plus the exchange term taken as a zero-range pseudo-potential is adopted. The zero-range pseudo-potential is added to account for the effect of knock-on exchange and to probe the reaction in non-elastic channels. Following this prescription, the B3Y-Fetal effective interaction is expressed in the standard form as [23],

$$V_{NN}(r) = \left[7419.23\frac{\mathrm{e}^{-4r}}{4r} - 1823.98\frac{\mathrm{e}^{-2.5r}}{2.5r}\right] + \hat{J}(E)\delta(r), \tag{2}$$

where $\hat{J}(E)\delta(r)$ is the zero-range pseudo-potential which accounts for the exchange part of the effective interaction [24]. The magnitude of $\hat{J}(E)$ is taken from [23] and the result is expressed as $\hat{J}(E) = -361\left[1 - 0.005\left(\frac{E}{A}\right)\right]$. In this study, the nuclear densities of the projectile and target nuclei used in Equation (1) are described using the two parameter Fermi-type function of the form [15] [25],

$$\rho(r) = \rho_0\left[1 + \exp\left(\frac{r - c}{a}\right)\right]^{-1} \tag{3}$$

where ρ_0, c, and a are the nuclear matter density parameters [26].

According to [27] [28], the bare NN interaction alone failed to reproduce nuclear matter properties at the correct binding energy of ≈−16 MeV. The inability of the bare NN interaction to reproduce nuclear matter properties at this binding energy necessitated the need to include a density dependence factor $f(\rho)$ into the original NN interaction to ensure saturation [28]. The density dependence factor $f(\rho)$ is added in the form [29] [30],

$$V_{D(Ex)}(\rho, r) = f(\rho)V_{D(Ex)}(r). \tag{4}$$

where $V_{D(Ex)}$ are the direct and exchange part of the effective NN interaction.

The explicit form of $f(\rho)$ under consideration has the form prescribed by [30]

$$f(\rho) = C\left(1+\alpha\exp\left(-\beta\rho\right)\right) \tag{5}$$

where ρ is the density at the saturation condition and C, α, and β are constants. The constants C, α, and β are taken from [23].

The optical potential of the present work is taken in the conventional form to be composed of a real and imaginary part. The imaginary part of the potential is chosen to be the same as the real part but multiplied by a different renormalization factor in a manner consistent with the prescription in [31],

$$U^{DF} = \left(N_r + iN_i\right)V_F\left(r\right) \tag{6}$$

where N_r and N_i are respectively, the real and imaginary renormalisation factors. The renormalisation factors are included to optimize the fit of the theoretical calculations and the experimental data.

The optical potential formulation of Equation (6) is modified to include the Woods-Saxon form factor plus Coulomb potential. The inclusion of the woods-Saxon form factor is necessitated for the need to determine the optical potential parameters in the inelastic scattering channel. The modified optical potential of Equation (6) is thus, written as,

$$U\left(r\right) = -\left[V\left(r\right)+iW\left(r\right)\right]+V_{Coul}\left(r\right), \tag{7}$$

where $V(r)$ and $W(r)$ are respectively the real and imaginary components of the optical potential and $V_{Coul}(r)$ is the Coulomb potential. The components of the nuclear optical potential are given by Ibraheem [16], and Khalaf *et al.* [32],

$$\left.\begin{aligned} V\left(r\right) &= V_0 f\left(r, R_v, a_v\right) \\ W\left(r\right) &= W_0 f\left(r, R_w, a_w\right) \end{aligned}\right\} \tag{8}$$

where V_0 and W_0 are respectively the strengths of the double folding potential, and $f(r, R_i, a_i)$ are the Woods-Saxon form factors. The Woods-Saxon form factor of Equation (8) is of the form [33]

$$f\left(r, R_i, a_i\right) = \left(1+\exp\left[\frac{r-R_i}{a_i}\right]\right)^{-1} \tag{9}$$

where $R_i = r_i A^{1/3}$ and a_i are the radius and the diffuseness parameters and A is the atomic mass number of the nuclei. The last term of Equation (7) corresponds to the Coulomb potential $V_{Coul}(r)$ and it is represented as [32]

$$V_{Coul}\left(r\right) = \begin{cases} \dfrac{Ze^2}{2R}\left(3-\dfrac{R^2}{R_C^2}\right), & R \le R_c \\ \dfrac{Ze^2}{R}, & R \ge R_c \end{cases} \tag{10}$$

where Z is the proton number of the target nuclei and e is the electronic charge.

In this work, the inelastic scattering data are analyzed using the optical potential of Equation (7) in a deformed form. With this prescription, the real transi-

tion ($V_T(r)$) and imaginary transition ($W_T(r)$) potentials were obtained as the derivatives of the real and imaginary central potentials and are expressed as [34]

$$\left.\begin{aligned} V_T(r) &= -\delta_l^v \frac{\mathrm{d}V(r)}{\mathrm{d}r} \\ W_T(r) &= -\delta_l^w \frac{\mathrm{d}W(r)}{\mathrm{d}r} \\ V_{TCoul}(r) &= \beta_{Coul} \frac{3Z_1Z_2e^2R_C^l}{(2l+1)r^{l+1}} \end{aligned}\right\} \tag{11}$$

where $V_{TCoul}(r)$ is the Coulomb transition potential, $\delta_l^{v(w)} = \beta_l R_i A_s^{1/3}$ are the potential deformation length, and β_l and β_{Coul} are respectively the ground-state (nuclear) and Coulomb deformation parameters.

2.2. Distorted Wave Born Approximations (DWBA)

In the DWBA, the transition amplitude used to calculate the inelastic differential cross sections is defined as [35] [36] [37],

$$T = \boldsymbol{J}\int \mathrm{d}^3r_b \int \mathrm{d}^3r_a \chi_{kf}^{(-)*}(\boldsymbol{r}_b)\langle bB|V|aA\rangle \chi_{kf}^{(+)}(\boldsymbol{r}_a), \tag{12}$$

where $\chi^{(-)}$ and $\chi^{(+)}$ are the distorted waves, $\boldsymbol{r}_a$ and $\boldsymbol{r}_b$ are the relative coordinates for the reaction of the type $A(a.b)B$ in the entrance (a,A) and (b,B) the exit channel, and $\boldsymbol{J}$ is the Jacobian for the transformation to the coordinates $\boldsymbol{r}_a$ and $\boldsymbol{r}_b$. The quantity $\langle bB|V|aA\rangle$ is the form factor for the reaction and it contains information about the nuclear structure.

The asymptotics of the distorted waves $\chi^{(\pm)}(\boldsymbol{k},\boldsymbol{r})$ requires that, the waves are plane waves of momentum $\boldsymbol{k}$ plus an outgoing (or incoming) spherical scattered wave. In the absence of Coulomb potential, the scattered waves are of the form [36],

$$\chi^{(\pm)}(\boldsymbol{k},\boldsymbol{r}) \to \mathrm{e}^{i\boldsymbol{k}\cdot\boldsymbol{r}} + f(\theta)\frac{\mathrm{e}^{\pm i\boldsymbol{k}\cdot\boldsymbol{r}}}{r} \tag{13}$$

Using partial wave analysis, the distorted wave functions are decomposed into partial waves and the radial part of the distorted waves is made to satisfy the equation,

$$\left\{\frac{\mathrm{d}^2}{\mathrm{d}r^2} + k^2 - \frac{L(L+1)}{r^2} - \frac{2\mu}{\hbar^2}\left[U(r) + U_c(r) + U_{Ls}(r)L\cdot s\right]\right\}\chi_{JLs}(k,r) = 0 \tag{14}$$

where $U(r)$ is the nuclear potential with real and imaginary parts, $U_c(r)$ is a Coulomb potential, $U_{Ls}(r)$ is a spin-orbit potential, and $\chi_{JLs}(k,r)$ is the radial wave function. The radial functions $\chi_{JLs}(k,r)$ satisfy the boundary conditions $\chi_{JLs}(k,r) = 0$ at the origin. At large values r for which the nuclear force may be neglected, the radial wave function is given by [35],

$$\chi_{JLs}(k,r) \to \frac{i}{2}\left[H_L^-(kr) - \eta_L^J H_L^+(kr)\right]\mathrm{e}^{i\sigma_L} \tag{15}$$

where $H_L^{\pm}(kr) = G_L(kr) \pm iF_L(kr)$ are the outgoing (+) and the incoming (−) Coulomb waves, η_L^J is the elastic scattering S-matrix and σ_L is the Coulomb phase shift.

The differential cross-section of the inelastic scattering using the DWBA of the DWUCK4 code is expressed in terms of the reaction strengths and summed over the spin indices as [11] [35] [36]

$$\frac{\mathrm{d}\sigma}{\mathrm{d}\Omega}(\theta) = \frac{2J_B+1}{2J_A+1}\frac{2l+1}{2j+1}\left|B_{lsj}\right|^2 \sigma_{DW}^{lsj}(\theta) \tag{16}$$

where $\sigma_{DW}^{lsj}(\theta)$ is defined as

$$\sigma_{DW}^{lsj}(\theta) = \frac{10}{4\pi}\frac{1}{E_a E_b}\frac{k_a}{k_b}\frac{1}{2s_a+1}\sum_{mm_a m_b}\left|\sum_{lsj} T_{lsj}^{mm_a m_b}\right|^2 \tag{17}$$

where $E_{a(b)}$ and are $k_{a(b)}$ the centre of mass energies and the wave numbers in the entrance and exit channels respectively. The strength of the interaction B_{lsj} is defined as

$$B_{lsj} = \left(\frac{2s+1}{2s_a+1}\right)^{1/2} A_{lsj} \tag{18}$$

The transition amplitude of Equation (17) is transformed as [36],

$$T^{M_A M_B; m_a m_b} = \frac{\sqrt{4\pi}}{k_\alpha k_\beta}\sum_{l,s,j}\sqrt{2l+1}B_{lsj} \times \left\langle J_A j M_A M_B - M_A \middle| J_B M_B \right\rangle S_{lsj}^{mm_a m_b} \tag{19}$$

where $k_{\alpha(\beta)}$ are the wave number in the entrance and the exit channels and S is the angle-dependent amplitude which is written as,

$$S_{lsj}^{mm_a m_b} = \sum_{Lb} \beta_{lsj;L_b}^{mm_a m_b} P_{L_b}^{m_a - m - m_b} \tag{20}$$

3. Procedure

The analysis of the deuteron-nucleus inelastic scattering data was carried out using the following computational procedure:

i) The calculated potentials in the elastic scattering channel using the double folding procedure of [23] were analyzed to find appropriate Woods-Saxon form factor parameters in the OM search code of the NRV. The search was carried out to optimize the Woods-Saxon form factor parameters. The potentials obtained were fitted to the Woods-Saxon form factor of Equation (9) to obtain the OP parameters for the various reactions [38].

ii) The optical potentials and Woods-Saxon form factor parameters were used as input parameters for the DWBA calculations in the inelastic channel.

iii) The optical potential and its corresponding Woods-Saxon form factor parameters were set to be the same in both the entrance and exit channels of the inelastic scattering.

iv) With the input data, β_l and β_{Coul} as included in Equation (11) are adjusted to fit the experimental data of the inelastic scattering cross-sections.

4. Results and Discussion

The analysis of the ground state scattering of deuteron from ^{58}Ni at 170 MeV, ^{70,72}Ge, ^{90}Zr, ^{116}Sn at 171 MeV and ^{208}Pb at 86 MeV was performed using the double folding model framework. The optical potentials determined using the DFM are taken from [23] and are fitted to corresponding Woods-Saxon form factor parameters in the search code of the NRV [39]. The best fit parameters are listed in **Table 1**.

The fits of the elastic scattering differential cross sections are presented in **Figures 1-6**. The solid lines in **Figures 1-6** correspond to the result of the theoretical calculations while the solid dots are those of the experimental data taken from [40] [41] [42]. From these figures, it can be deduced that the double folding potentials successfully described the angular distributions of the elastic scattering differential cross-section over all the measured angular ranges at all energies.

Table 1. Best fit OP parameters of deuteron elastic scattering on different nuclei.

Reaction	E_{lab} (MeV)	V_R	r_v	a_v	W_I	r_w	a_w
d + ^{58}Ni	170	96	0.77	1.15	73	0.97	0.72
d + ^{70}Ge	171	100	0.67	1.15	60	0.61	1.07
d + ^{72}Ge	171	105	0.78	0.95	90	0.80	0.90
d + ^{90}Zr	171	110	0.73	1.17	75	0.90	0.85
d + ^{116}Sn	171	150	0.81	0.99	120	0.82	0.90
d + ^{208}Pb	86	214	0.54	1.34	83	0.97	0.85

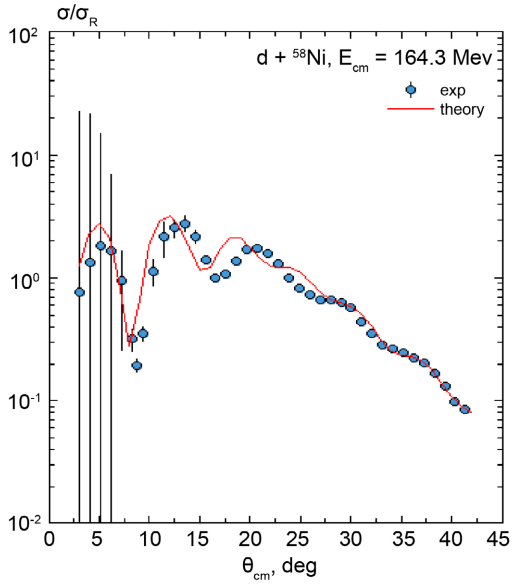

Figure 1. Elastic scattering angular distribution of d + ^{58}Ni at $E_{lab} = 170$ MeV.

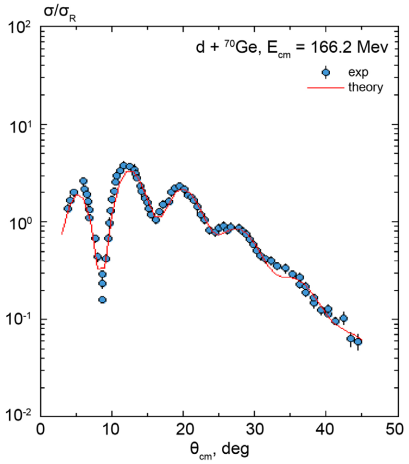

Figure 2. Elastic scattering angular distribution of $d + {}^{70}\mathrm{Ge}$ at $E_{lab} = 171\,\mathrm{MeV}$.

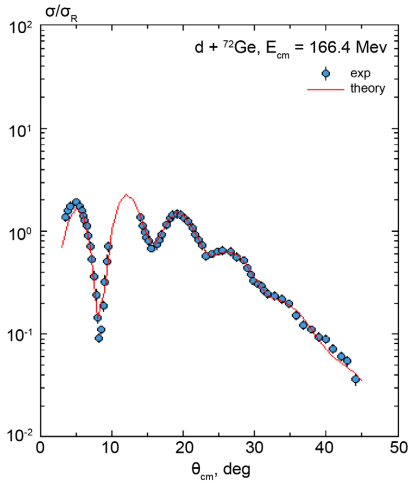

Figure 3. Elastic scattering angular distribution of $d + {}^{72}\mathrm{Ge}$ at $E_{lab} = 171\,\mathrm{MeV}$.

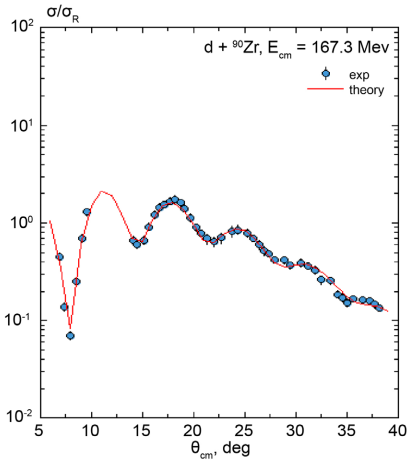

Figure 4. Elastic scattering angular distribution of $d + {}^{90}\mathrm{Zr}$ at $E_{lab} = 171\,\mathrm{MeV}$.

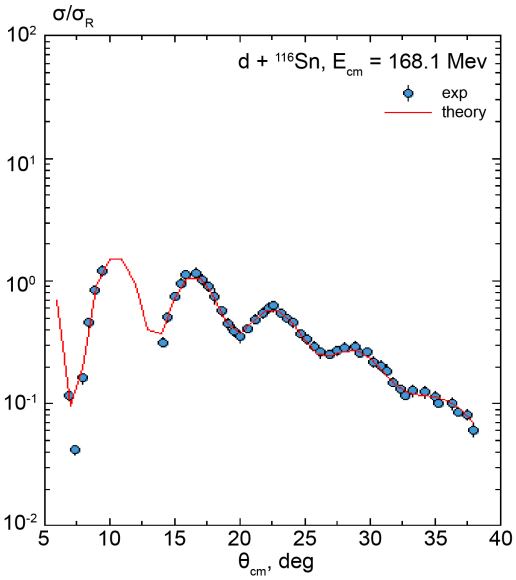

Figure 5. Elastic scattering angular distribution of $d + {}^{116}Sn$ at $E_{lab} = 171\,\text{MeV}$.

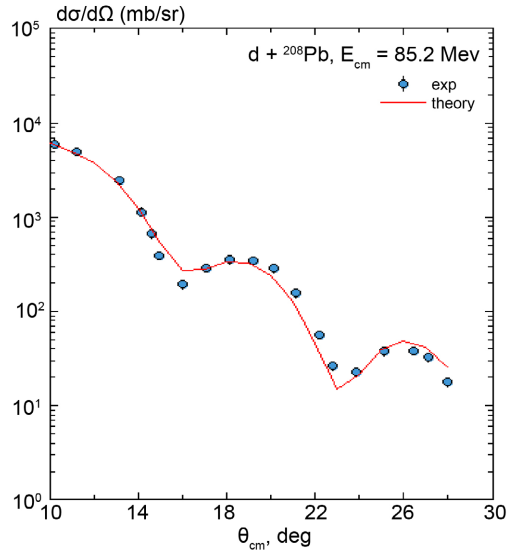

Figure 6. Elastic scattering angular distribution of $d + {}^{208}Pb$ at $E_{lab} = 86\,\text{MeV}$.

The analysis of the excited states of the deuteron inelastic scattering from ^{58}Ni (2^+), ^{70}Ge (2^+), ^{72}Ge (2^+), ^{90}Zr (2^+), ^{116}Sn (2^+), and ^{208}Pb (5^-) was performed with the help of the DWUCK4 code [36] which is available via the internet on the site of the NRV project [43]. A comparison of the theoretical calculations and the experimental data was made and the results are presented in **Figures 7-12**. The DWBA calculations were made using the parameters listed in **Table 1** as input parameters in both the entrance and exit channels. The inelastic scattering cross-sections are evaluated using the transition potentials of Equation (11). The fit of the theoretical calculations to the experimental data was done by adjusting

the ground-state β_l and Coulomb β_{Coul} deformation form factors. The best-fit parameters for the inelastic scattering analysis are listed in Table 2.

The measurement of the inelastic scattering cross-section data of deuteron scattering from ^{58}Ni (2^+), ^{70}Ge (2^+), ^{72}Ge (2^+), ^{90}Zr (2^+), ^{116}Sn (2^+), and ^{208}Pb (5^-) leading to the corresponding excited state are shown in Figures 7-12. The solid symbols represent the experimental data which are taken from [40] [41] [42] and the solid lines are the result of the present calculations using the DWUCK4 code [36]. The obtained diffraction patterns of the angular distributions of the deuteron scattering to the excited states of the various reactions listed in Table 2 were found to be consistent with the corresponding observed data. In the fitting process, the strength of the folded potential of ^{58}Ni (2^+) was adjusted by 0.1% to obtain the Woods-Saxon form factor parameters. The fits were found to be in good agreement with experimental data and other calculations as reported in [15] [16]. In general, the observed diffraction patterns were well reproduced by the theoretical calculations. The fit of the excited states was achieved by using the deformation parameters listed in Table 2.

Table 2. Best fit parameters of deuteron inelastic scattering on different nuclei.

Reaction	E_{lab} (MeV)	States	β_l	β_{Coul}
d + ^{58}Ni	170	2^+	0.23	0.30
d + ^{70}Ge	171	2^+	0.40	0.80
d + ^{72}Ge	171	2^+	0.36	0.80
d + ^{90}Zr	171	2^+	0.17	0.50
d + ^{116}Sn	171	2^+	0.18	0.10
d + ^{208}Pb	86	5^-	0.15	1.00

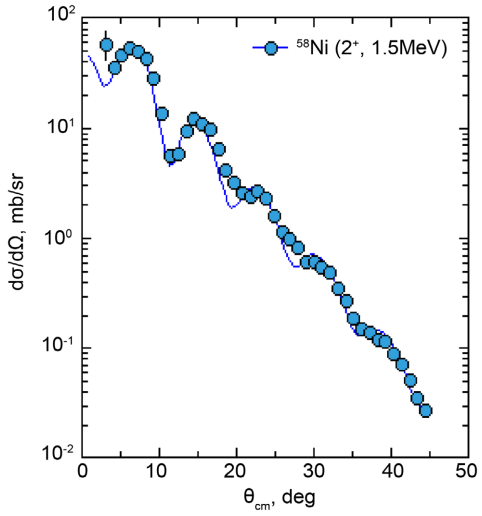

Figure 7. Angular distribution data of the excited (2^+) state of deuteron scattering from ^{58}Ni at 170 MeV.

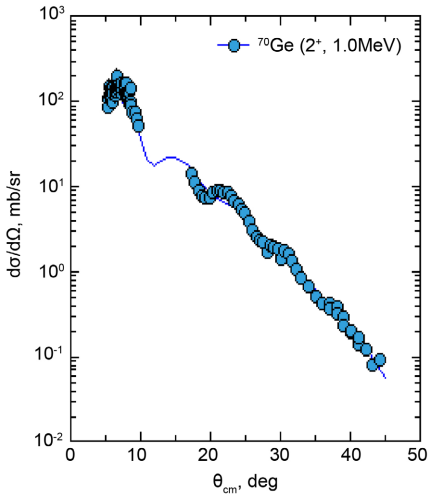

Figure 8. Angular distribution data of the excited (2^+) state of deuteron scattering from ^{70}Ge at 171 MeV.

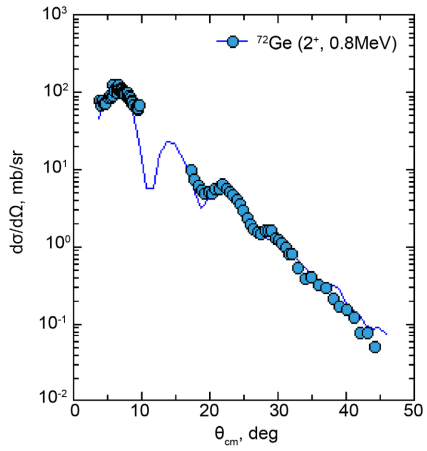

Figure 9. Angular distribution data of the excited (2^+) state of deuteron scattering from ^{72}Ge at 171 MeV.

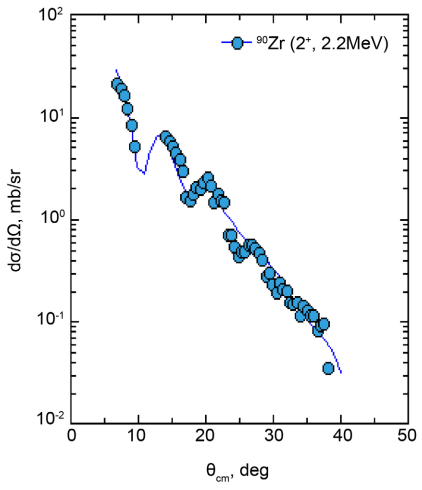

Figure 10. Angular distribution data of the excited (2^+) state of deuteron scattering from ^{90}Zr at 171 MeV.

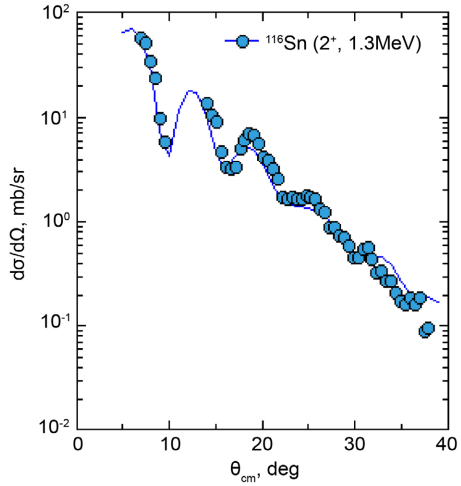

Figure 11. Angular distribution data of the excited (2^+) state of deuteron scattering from ^{116}Sn at 171 MeV.

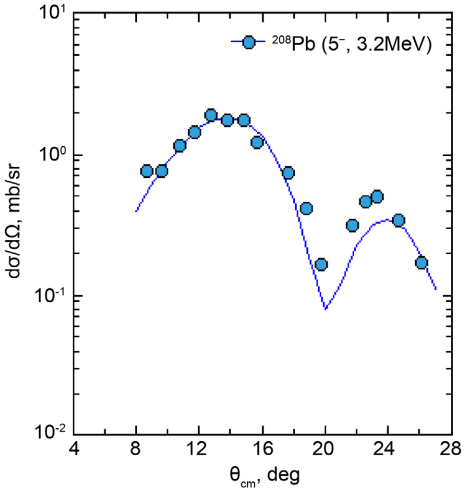

Figure 12. Angular distribution data of the excited (5^-) state of deuteron scattering from ^{208}Pb at 86 MeV.

5. Conclusion

This work analyzed the inelastic scattering data of deuteron from different target nuclei namely: ^{58}Ni, ^{70,72}Ge, ^{90}Zr, ^{116}Sn, and ^{208}Pb at different energies using the optical model framework. The B3Y-Fetal effective interaction was used in the double folding model to determine the strength of the optical potentials and the corresponding optical parameters in the elastic channel. The extracted potentials of the DFM were used to fit the optical parameters for the inelastic scattering analysis. An apparent success to describe the inelastic scattering data was achieved using the DWBA of the DWUCK4 code. The results of the present calculations compare quite well with the corresponding experimental data. The good agreement seen in the fit of the angular distribution data of the inelastic scattering calculation is a reflection of the appropriateness of the B3Y-Fetal interaction, the double folding model and the DWBA calculations to the descrip-

tion of scattering cross-section data in both the elastic and inelastic channels. The success achieved in this work may encourage researchers to extend this formalism to the analysis of nuclear reactions in other nonelastic channels.

Acknowledgements

The authors wish to thank Dr. Andrey S. Denikin (Head of the Theoretical and Computational Group of Flerov Laboratory of Nuclear Reactions, JINR) and Prof. Alexander V. Karpov (JINR) for valuable discussions and comments.

Conflicts of Interest

The authors declare no conflicts of interest.

References

[1] El-Hammamy, M.N. (2015) Double Folding Analysis of ^{3}H Elastic and Inelastic Scattering to Low Lying States on ^{90}Zr, ^{116}Sn and ^{208}Pb at 270 MeV. *Chinese Physics C*, **39**, Article ID: 034101. https://doi.org/10.1088/1674-1137/39/3/034101

[2] Amer, A.H., Penionzhkevich, Y.E., Ibraheem, A.A. and Hamada, S. (2020) Comparison between the Elastic Scattering of ^{12}C(α, α)^{12}C and ^{12}C(^{6}He, ^{6}He)^{12}C Different Nuclear Potentials. *International Journal of Modern Physics E*, **29**, Article ID: 2050086. https://doi.org/10.1142/S021830132050086X

[3] Farid, M.E. and Hassanain, M.A. (2004) Folding Model and Coupled-Channels Analysis of ^{6,7}Li Elastic and Inelastic Scattering. *The European Physical Journal A*, **19**, 231-236. https://doi.org/10.1140/epja/i2003-10122-3

[4] Amer, A.H., Amar, A., Hamada, S. and Bondouk, I.I. (2016) Optical and Double Folding Model Analysis for Alpha Particles Elastically Scattered from ^{9}Be and ^{11}B Nuclei at Different Energies. *World Academy of Science, Engineering and Technology, International Journal of Chemical and Molecular Engineering*, **10**, 161-166.

[5] Hamada, S., Burtebayev, N., Amangeldi, N. and Amar, A. (2011) Detailed Phenomenological Study of ^{14}N Elastically Scattered on ^{12}C in a Wide Energy Range. *World Academy of Science, Engineering and Technology, International Journal of Chemical and Molecular Engineering*, **5**, 110-112.

[6] Sert, Y., Yegin, R. and Dogan, H. (2015) A Theoretical Investigation of ^{9}Be + ^{27}Al Reaction: Phenomenological and Microscopic Model Approximation. *Indian Journal of Physics*, **89**, 1093-1100. https://doi.org/10.1007/s12648-015-0685-9

[7] Perey, C.M. and Perey, F.G. (1974) Compilation of Phenomenological Optical-Model Parameters 1969-1972. *Atomic Data and Nuclear Data Tables*, **13**, 293-337. https://doi.org/10.1016/0092-640X(74)90005-9

[8] Farid, M.E., Mahmoud, Z.M.M. and Hassan, G.S. (2001) Analysis of Heavy Ions Elastic Scattering Using the Double Folding Cluster Model. *Nuclear Physics A*, **691**, 671-690. https://doi.org/10.1016/S0375-9474(01)00587-5

[9] Farid, M.E. (2001) Double Folding Cluster Optical Potential of Heavy Ions Interaction. 3*rd Conference on Nuclear & Particle Physics* (*NUPPAC* 01), Cairo, 20-24 October 2001, 217-222. https://doi.org/10.1007/s13538-015-0354-7

[10] Paulo, S., Hassanain, M.A. and Ibraheem, A.A. (2015) Study of the Elastic Scattering of ^{32}S by ^{24}Mg at Low Energies. *Brazilian Journal of Physics*, **45**, 699-707.

[11] Satchler, G.R. (1983) Direct Nuclear Reactions. Oxford University Press, Oxford.

[12] Behairy, K., Mahmoud, Z.M.M. and Hassanain, M.A. (2015) Elastic and Inelastic α-Scatterings from ^{58}Ni, ^{116}Sn, and ^{208}Pb Targets at 288, 340, 480, and 699 MeV. *Brazilian Journal of Physics*, **45**, 673-686. https://doi.org/10.1007/s13538-015-0351-x

[13] Farid, M.E., Alsagheer, L., Alharbi, W.R. and Ibraheem, A.A. (2014) Analysis of Deuteron Elastic Scattering in the Framework of the Double Folding Optical Potential Model. *Life Science Journal*, **11**, 208-216.

[14] Attia, A., El-Akkad, F.A., Nasr, M., El-Nohy, N. and Abdel-Moneim, A.M. (2010) Form Factor Calculation for (^{16}O + ^{16}O), (^{12}C + ^{12}C) and (^{12}C + ^{24}Mg) at Intermediate Energies. 10*th Radiation Physics & Protection Conference*, Cairo, 27-30 November 2010, 381-390.

[15] El-Attar, A.L., Farid, M.E. and El-Aref, M.G. (2008) Optical Model Analyses of Deuteron Inelastic Scattering. 9*th International Conference for Nuclear Sciences and Applications*, Sharm Al Sheikh, 11-14 February 2008, 1239.

[16] Ibraheem, A.A. (2016) Analysis of Deuteron-Nucleus Scattering Using Sao Paulo Potential. *Brazilian Journal of Physics*, **46**, 746-753. https://doi.org/10.1007/s13538-016-0453-0

[17] Hagino, K., Takehi, T. and Takigawa, N. (2006) No-Recoil Approximation to the Knock-On Exchange Potential in the Double Folding Model for Heavy-Ion Collisions. *Physical Review C—Nuclear Physics*, **74**, Article ID: 037601. https://doi.org/10.1103/PhysRevC.74.037601

[18] Satchler, G.R. and Love, W.G. (1979) Folding Model Potentials from Realistic Interactions for Heavy-Ion Scattering. *Phys. Reports* (*Review Section of Physics Letters*), **55**, 183-254. https://doi.org/10.1016/0370-1573(79)90081-4

[19] Brandan, M.E. and Satchler, G.R. (1997) The Interaction between Light Heavy-Ions and What It Tells Us. *Physics Reports*, **285**, 143-243. https://doi.org/10.1016/S0370-1573(96)00048-8

[20] Fiase, J.O., Devan, K.R.S. and Hosaka, A. (2002) Mass Dependence of M3Y-Type Interactions and the Effects of Tensor Correlations. *Physical Review C—Nuclear Physics*, **66**, Article ID: 014004. https://doi.org/10.1103/PhysRevC.66.014004

[21] Ochala, I. and Fiase, J.O. (2018) Symmetric Nuclear Matter Calculations: A Variational Approach. *Physical Review C*, **98**, Article ID: 064001. https://doi.org/10.1103/PhysRevC.98.064001

[22] Abenga, R.C., Fiase, J.O. and Ibeh, G.J. (2020) Optical Model Analysis of α + ^{40}Ca at E_{lab} = 104 and 141.7 MeV Using a Mass-Dependent M3Y-Type Effective Interaction. *Nigerian Annals of Pure and Applied Sciences*, **3**, 252-260. https://doi.org/10.46912/napas.144

[23] Abenga, R.C., Yahaya, Y.I. and Adamu, I.D. (2021) Double Folding Potential of Deuteron Elastic Scattering on Target Nuclei in the Mass Range of 50 ≤ A ≤ 208 Using a Mass-Dependent Effective Interaction. *Bayero Journal of Physics and Mathematical Science*, **1**, 1-14.

[24] Modarres, M. and Rahmat, M. (2015) The LOCV Averaged Two-Nucleon Interactions versus the Density-Dependent M3Y Potential for the Heavy-Ion Collisions. *Nuclear Physics A*, **934**, 148-166. https://doi.org/10.1016/j.nuclphysa.2014.11.006

[25] Satchler, G.R. (1994) A Simple Effective Interaction for Peripheral Heavy-Ion Collisions at Intermediate Energies. *Nuclear Physics A*, **579**, 241-255. https://doi.org/10.1016/0375-9474(94)90804-4

[26] De Vries, H., De Jager, C.W. and De Vries, C. (1987) Charge-Density-Distribution Parameters from Elastic Electron Scattering. *Atomic Data and Nuclear Data Tables*,

36, 495-536. https://doi.org/10.1016/0092-640X(87)90013-1

[27] Seif, W.M. (2011) Nuclear Matter Equation of State Using Density-Dependent M3Y Nucleon-Nucleon Interactions. *Journal of Physics G*: *Nuclear and Particle Physics*, **38**, Article ID: 035102. https://doi.org/10.1088/0954-3899/38/3/035102

[28] Khoa, D.T., Von Oertzen, W. and Ogloblin, A.A. (1996) Study of the Equation of State for Asymmetric Nuclear Matter and Interaction Potential between Neutron-Rich Nuclei Using the Density-Dependent M3Y Interaction. *Nuclear Physics A*, **602**, 98-132. https://doi.org/10.1016/0375-9474(96)00091-7

[29] Khoa, D.T. and Von Oertzen, W. (1993) A Nuclear Matter Study Using the Density Dependent M3Y Interaction. *Physics Letters B*, **304**, 8-16. https://doi.org/10.1016/0370-2693(93)91391-Y

[30] Moharram, S.A. and El-Shal, A.O. (2002) Spin Polarized Cold and Hot Dense Neutron Matter. *Turkish Journal of Physics*, **26**, 167-177.

[31] Hanna, K.M., Lukyanov, K.V., Lukyanov, V.K., Metawei, Z., Slowinski, B. and Zemlyanaya, E.V. (2005) Excitation of Nuclear Collective Semi-Microscopic Optical Potential. 5*th Conference on Nuclear and Particle Physics*, Cairo, 19-23 November 2005, 155-164.

[32] Khalaf, A.M., Khalifa, M.M., Solieman, A.H.M. and Comsan, M.N.H. (2017) Nuclear Matter Parameters and Optical Model Analysis of Proton Elastic Scattering on the Doubly Magic Nucleus ^{40}Ca. *Nuclear Physics A*, **939**, 83-93. https://doi.org/10.1016/j.nuclphysa.2017.09.009

[33] An, H. and Cai, C. (2006) Global Deuteron Optical Model Potential for the Energy Range Up to 183 MeV. *Physical Review C—Nuclear Physics*, **73**, Article ID: 054605. https://doi.org/10.1103/PhysRevC.73.054605

[34] Clark, H.L., Lui, Y.W. and Youngblood, D.H. (1998) Folding Model Analysis of the Excitation of Low-Lying States and the High Energy Octupole Resonance in ^{116}Sn by 240 MeV α Scattering. *Physical Review C*, **57**, 2887-2891. https://doi.org/10.1103/PhysRevC.57.2887

[35] Karpov, A.V., *et al.* (2017) NRV Web Knowledge Base on Low-Energy Nuclear Physics. *Nuclear Instruments and Methods in Physics Research Section A*: *Accelerators*, *Spectrometers*, *Detectors and Associated Equipment*, **859**, 112-124. https://doi.org/10.1016/j.nima.2017.01.069

[36] Langanke, K., Maruhn, J.A. and Koonin, S.E. (1993) Computational Nuclear Physics 2. Nuclear Reactions. Springer-Verlag, Berlin. https://doi.org/10.1007/978-1-4613-9335-1

[37] Karpov, A.V. and Saiko, V.V. (2017) Modeling Near-Barrier Collisions of Heavy Ions Based on a Langevin-Type Approach. *Physical Review C*, **96**, Article ID: 024618. https://doi.org/10.1103/PhysRevC.96.024618

[38] Denisov, V.Y. and Davidovskaya, O.I. (2010) Elastic Scattering of Heavy Ions and Nucleus-Nucleus Potential with a Repulsive Core. *Bulletin of the Russian Academy of Sciences*: *Physics*, **74**, 572-576. https://doi.org/10.3103/S1062873810040325

[39] Zagrebaev, V., Denikin, A. and Alekseev, A. (2000) Optical Model of Elastic Scattering. Nuclear Reaction Video Project. http://nrv.jinr.ru/nrv

[40] Morsch, H.P., Sukosd, C., Rogge, M., Turek, P. and Machner, H. (1980) Giant Monopole and Quadrupole Resonances and Other Multipole Excitations in ^{208}Pb Studied in 43 MeV/Nucleon Alpha-Particle and Deuteron Scattering. *Physical Review C*, **22**, 489-500. https://doi.org/10.1103/PhysRevC.22.489

[41] Bäumer, C., *et al.* (2001) Deuteron Elastic and Inelastic Scattering from ^{12}C, ^{24}Mg,

and ^{58}Ni at 170 MeV. *Physical Review C—Nuclear Physics*, **63**, 376011-376014. https://doi.org/10.1103/PhysRevC.63.037601

[42] Korff, A., *et al.* (2004) Deuteron Elastic and Inelastic Scattering at Intermediate Energies from Nuclei in the Mass Range 6 ≤ A ≤ 116. *Physical Review C*, **70**, Article ID: 067601.

[43] Zagrebaev, V., Denikin, A. and Alekseev, A. (2009) DWBA for Inelastic Reactions. Nuclear Reaction Video Project. http://nrv.jinr.ru/nrv